Redox Biology 1 (2013) 599–607

Contents lists available at ScienceDirect

Redox Biology

journal homepage: www.elsevier.com/locate/redox

Research Paper

Superoxide dismutase mimic, MnTE-2-PyP^{5+} ameliorates acute and chronic proctitis following focal proton irradiation of the rat rectum

John O. Archambeau [a], Artak Tovmasyan [b], Robert D. Pearlstein [c,*], James D. Crapo [d], Ines Batinic-Haberle [b,**]

[a] Department of Radiation Medicine, Loma Linda University, Loma Linda, CA, USA
[b] Department of Radiation Oncology, Duke University School of Medicine, Durham, NC 27710, USA
[c] Department of Surgery (Neurosurgery), Duke University School of Medicine, Durham, NC 27710, USA
[d] Department of Medicine, Division of Pulmonary, Critical Care and Sleep Medicine, Denver, CO 80206, USA

ARTICLE INFO

Article history:
Received 17 September 2013
Received in revised form
12 October 2013
Accepted 14 October 2013

Keywords:
SOD mimic
Mn porphyrin
MnTE-2-PyP^{5+}
Radioprotector
Radiation proctitis
Proton beam therapy

ABSTRACT

Radiation proctitis, an inflammation and damage to the lower part of colon, is a common adverse event of the radiotherapy of tumors in the abdominal and pelvic region (colon, prostate, cervical). Several Mn(III) porphyrin-based superoxide dismutase mimics have been synthesized and successfully evaluated in preclinical models as radioprotectants. Here we report for the first time the remarkable rectal radioprotection of frequently explored Mn(III) *meso*-tetrakis(*N*-ethylpyridinium-2-yl)porphyrin, MnTE-2-PyP^{5+}. A batch prepared in compliance with good manufacturing practice (GMP), which has good safety/toxicity profile, was used for this study. MnTE-2-PyP^{5+} was given subcutaneously at 5 mg/kg, either 1 h before or 1 h after irradiation, with additional drug administered at weekly intervals thereafter. MnTE-2-PyP^{5+} ameliorated both acute and chronic radiation proctitis in male Sprague-Dawley rats irradiated with 20–30 Gy protons delivered to 2.5 cm span of rectum using spread-out Bragg peak of a proton treatment beam. Focal irradiation of the rectum produced acute proctitis, which healed, followed by chronic rectal dilation and symptomatic proctitis. MnTE-2-PyP^{5+} protected rectal mucosa from radiation-induced crypt loss measured 10 days post-irradiation. Significant effects were observed with both pre- and post-treatment regimens. However, only MnTE-2-PyP^{5+} pre-treatment, but not post-treatment, prevented the development of rectal dilation, indicating that proper dosing regimen is critical for radioprotection. The pre-treatment also prevented or delayed the development of chronic proctitis depending on the radiation dose. Further work aimed at developing MnTE-2-PyP^{5+} and similar drugs as adjunctive agents for radiotherapy of pelvic tumors is warranted. The present study substantiates the prospects of employing this and similar analogs in preserving normal tissue during cancer radiation as well as any other radiation exposure.

Introduction

Radiation is a cost-effective treatment, and plays central role in cancer treatment and is a major cure for 25% of all cancers [1]. Yearly, over 200,000 patients receive abdominal or pelvic radiation therapy, and the estimated number of cancer survivors with post-radiation intestinal dysfunction is 1.5–2 million [2]. The risk of injury to the intestine is dose limiting during the radiation therapy of abdominal and pelvic region such as in the treatments of colon, cervical and prostate cancers. Delayed bowel toxicity is difficult to manage and adversely impacts the quality of life of cancer survivors. Worthwhile progress towards reducing toxicity of radiation therapy has been made by dose-sculpting treatment techniques. The radiation damage to the gastrointestinal (GI) tract is a concern in both clinical practice and in the context of accidental radiological exposures and nuclear terrorist attacks [1,3–6]. Recent study showed that 47% of women who received

Abbreviations: SOD, superoxide dismutase; MnP, Mn(III) porphyrins; MnTE-2-PyP^{5+}, Mn(III) *meso*-tetrakis(*N*-ethylpyridinium-2-yl)porphyrin (AEOL10113, BMX-010); MnTM-2-PyP^{5+}, Mn(III) *meso*-tetrakis(*N*-methylpyridinium-2-yl)porphyrin (AEOL10112); MnTnHex-2-PyP^{5+}, Mn(III) *meso*-tetrakis(*N*-n-hexylpyridinium-2-yl) porphyrin (BMX-001); MnTnBuOE-2-PyP^{5+}, Mn(III) *meso*-tetrakis(*N*-n-butoxyethylpyridinium-2-yl)porphyrin; MnTDE-2-ImP^{5+}, Mn(III) *meso*-tetrakis(*N,N'*-diethylimidazolium-2-yl)porphyrin (AEOL10150); HIF-1α, hypoxia inducible factor-1; NF-κB, nuclear factor κB; SP-1, specificity protein-1; AP-1, activator protein-1; TF, transcription factor; GSH, glutathione; $k_{cat}(O_2^{\cdot-})$, the rate constant for the catalysis of $O_2^{\cdot-}$ dismutation by Mn porphyrin or SOD enzyme; CGE, cobalt gray equivalent; PT, proton therapy

* Correspondence to: Departments of Surgery (Neurosurgery), Duke University School of Medicine, Durham, NC 27710, USA.
** Corresponding author. Tel.: +91 96842101; fax: +91 96848718.
E-mail addresses: robert.pearlstein@duke.edu (R.D. Pearlstein), ibatinic@duke.edu (I. Batinic-Haberle).

2213-2317
http://dx.doi.org/10.1016/j.redox.2013.10.002

radiotherapy for cervical or endometrial cancer reported symptoms of radiation-related intestinal injury within 3 months following therapy completion, which affected their quality of life [5]. These results are consistent with data from a survey showing that 53% of patients had reported that bowel symptoms significantly affect their quality of life, whilst 81% of patients described new-onset gastrointestinal problems after receiving radiotherapy [1,5].

Radiation proctitis, inflammation and damage to the lower parts of the colon, is a common adverse event associated with radiotherapy of tumors in the pelvic region; for review see Ref. [7]. It can arise as either an acute or late response to treatment (or both) [1,3–6]. The recent data on dose–volume effect in radiation induced rectal injury was reviewed by Michalski et al. [8] and by Shadad et al. [1,5]. Briefly, the acute symptoms, like nausea, vomiting, abdominal pain and diarrhea usually settle within three weeks after completion of radiotherapy [1]. Delayed effects usually follow progressive course starting at several months and up to several years after radiation. Those effects are: bowel toxicity, intermittent diarrhea, constipation due to altered colon motility (as a consequence of fibrosis and stricture formation), recurrent pain, and increased risk of obstruction or pseudo-obstruction secondary to fecal loading [1]. Excessive fibrosis can cause loss of ano-rectal compliance and manifests as urgency and frequency. Fecal incontinence has been reported in up to 20% of patients and significantly reduces patients' quality of life.

Different pathological processes contribute to the development of the acute and late responses and both are triggered by pro-inflammatory mediators released in response to reactive species formed in the GI epithelium during irradiation. Acute effects are also the result of mitotic inhibition or loss of crypt cells that populate the mucosal lining and result in disruption of the epithelial mucosa. Significant loss of epithelial mucosa, for example in accidental radiation exposure or nuclear terrorist attack in which a large fraction of the GI tract may be irradiated, can result in a life-threatening condition due to the loss of GI barrier and transport functions.

Animal models have been developed that mimic the adverse effects of GI irradiation observed clinically [9–14]. The general pattern observed in these studies include **(i)** an acute phase characterized by the loss of surface epithelial cells, crypt cells, and crypts, and **(ii)** a late phase that evolved during the subsequent 4–6 months following irradiation. The late phase at the higher dose range would eventuate in animal death from intestinal obstruction [15–17]. Around 20% of the animals in the Trott model of chronic proctitis died from hydronephrosis rather than radiation-induced GI complications due to unintended irradiation of the bladder/ureter [10,17]. The hydronephrosis, literally water in kidney, refers to the distension and dilation of the renal pelvis and calyces, usually caused by obstruction of the free flow of urine from the kidney. The radiosensitivity of the ureter was studied by Knowles and Trott, who showed that doses as low as 10 Gy delivered to the rat ureter (below the dose range used to produce chronic proctitis in rats) could produce hydronephrosis [18].

Proton beam therapy vs. X-ray treatment

One of the goals of the present study was to improve on earlier methods for irradiating the rat rectum by reducing the dose delivered to other organs using proton beams rather than X-rays. High energy proton beams stop abruptly in tissue at the end of their range, deposit most energy in tissues of interest and thus distribute dose in superior manner relative to X-rays [1]. Proton therapy (PT) is more densely ionizing along the treatment path allowing higher quantum energy and high linear energy transfer to kill cancer (see also Material and methods Section). It is a very promising modality for larger tumors which could be radiated at high doses without significant exposure of surrounding normal tissue. With hepatocellular carcinoma proton beam therapy was effective, safe and well tolerated in clinical studies. The relative biological effectiveness (RBE) in clinical practice for protons is 1.1; in turn the linear energy transfer (LET) is not much different over most of the treatment path in comparison to photon radiation. In clinical practice the PT is not considered a high LET treatment modality, e.g., like other higher mass particle beam therapy (e.g., carbon). The dose distribution still remains a major difference between the proton and conventional X-ray therapy. Although new X-ray technologies are pretty much identical to PT in

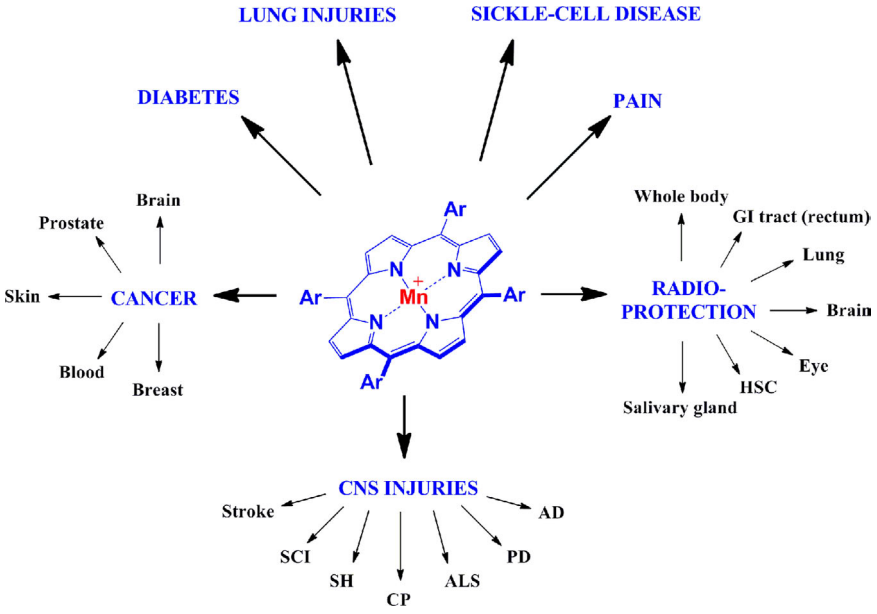

Fig. 1. Therapeutic effects of Mn porphyrins. Ar indicates *meso* (the bridge in between two pyrrolic rings) aromatic *either ortho N*-alkylpyridyl groups [alkyl being ethyl in MnTE-2-PyP^{5+} or n-hexyl in MnTnHex-2-PyP^{5+}], or *ortho N*-alkoxyalkylpyridyl substituents [alkoxyalkyl being n-butoxyethyl in MnTnBuOE-2-PyP^{5+}], or di-*ortho N,N'*-dialkylimidazolyl substituents [alkyl being ethyl in MnTDE-2-ImP^{5+}]. *Ortho* position is the position on pyridyl or imidazolyl rings closest to the *meso* position. SCI=spinal cord injury, SH=subarachnoid hemorrhage, CP=cerebral palsy, ALS=amyotrophic lateral sclerosis, PD=Parkinson's disease, AD=Alzheimer's disease, HSC=hematopoietic stem cells, GI=gastrointestinal tract. See for details on therapeutic effects in Refs. [21,44,45].

confining the dose in the vicinity of the target, PT offers reduced "integral dose" to normal tissue.

Mn(III) *meso*-tetrakis(*N*-ethylpyridinium-2-yl)porphyrin (MnTE-2-PyP^{5+}, AEOL10113, BMX-010) is a potent SOD mimic, peroxynitrite scavenger as well as scavenger of a number of other species [19–22]. The *meso* (the bridges between two pyrrolic units) positions (indicated as Ar, aromatic rings) in MnTE-2-PyP^{5+} are occupied with *N*-ethylpyridyl groups (Fig. 1). MnTE-2-PyP^{5+} was developed based on structure–activity relationship between the redox ability of metalloporphyrins described with metal-centered reduction potential, $E_{1/2}$ and their ability to dismute superoxide described by the rate constant for the catalysis of O_2^- dismutation, $k_{cat}(O_2^-)$ [21,23,24]. The log $k_{cat}(O_2^-)$ is 7.76 for MnTE-2-PyP^{5+} while 8.84–9.2 for SOD enzymes (see review [21] for details). The cationic charges in close vicinity of the metal site (*ortho* position) are critical for its SOD-like activity as they afford the thermodynamic and electrostatic facilitation for the approach of negatively charged superoxide, peroxynitrite and a number of other anionic species thought to be involved in the action of this compound, such as hypochlorite, monodeprotonated ascorbate, monodeprotonated hydrogen peroxide and thiolates [21]. The positive charges allow this and similar cationic compounds to accumulate in mitochondria and tissues rich in phospholipids, *i.e.* anionic phosphate groups [21]. MnTE-2-PyP^{5+} is among the most potent SOD mimics and peroxynitrite scavengers thus far reported and the most studied Mn porphyrin-based SOD mimic (see contributions to Forum Issue on "SOD therapeutics" in *Antioxid Redox Signaling*, also [21]). It has shown remarkable potency in numerous animal models of oxidative stress injuries [19]. The compound is also reactive towards simple thiols (GSH, L-cysteine, *N*-acetylcysteine) [21,25,26] and protein thiols which seems to be at least in part involved in its *in vivo* mechanism/s of action/s. It has been recently substantiated that in the presence of elevated H_2O_2 levels, the MnTE-2-PyP^{5+} would oxidize or S-glutathionylate (along with GSH) p65 and p50 subunits of master transcription pro-survival factor, NF-κB which would in turn suppress inflammatory pathways [27]. Such reactivites may be operative wherever excessive and cycling inflammation is involved [21]. Needless to say such thiol modifications by MnPs have pro-oxidative character, yet result in antioxidative effects – suppression of NF-κB activation, *i.e.* inflammation (see [21] for details on type of actions and related circumstances). In addition, the impact of MnTE-2-PyP^{5+} on AP-1, HIF-1α and SP-1 have been demonstrated [19–22,28]. Therefore, we recently prefer to regard this and similar compounds rather as redox-regulators of cellular transcriptional activities than as SOD mimics. Importantly, though, the magnitude of their SOD-like activity, described by $k_{cat}(O_2^-)$ parallels the magnitude of their therapeutic efficacy. Thus targeting SOD-like activity is still a valuable approach for developing potent redox-active drugs. MnTE-2-PyP^{5+} and related Mn porphyrin-based SOD mimics [such as Mn(III) *meso*-tetrakis(*N,N'*-diethylimidazolium-2-yl) porphyrin, MnTDE-2-ImP^{5+} (AEOL10150); Mn(III) *meso* tetrakis(*N*-methylpyridinium-2-yl)porphyrin, MnTM-2-PyP^{5+} (AEOL10112); and Mn(III) *meso* tetrakis(*N*-n-hexylpyridinium-2-yl)porphyrin, MnTnHex-2-PyP^{5+}] have been reported to protect normal lung [29,30], prostate [31–33], whole body [34,35], eye [28,36], salivary glands and brain tissue from radiation damage [21,29,37–41]. The accumulation of cationic Mn porphyrins, including MnTE-2-PyP^{5+} and MnTnHex-2-PyP^{5+} in mitochondria [21,42,43] contributes to their exceptional therapeutic efficacy in a variety of diseases indicated in Fig. 1, which all bear some components of the perturbance in physiological redox environment. The therapeutic effects of Mn porphyrins in different models of animal diseases are reviewed in details in Forum Issue on "SOD therapeutics" in *Antioxidants and Redox Signaling* [19,21,22,44,45].

A MnTE-2-PyP^{5+} batch, compliant with Good Manufacturing Practice, was synthesized and the data on its excellent safety/toxicity profile have been reported [9]. Whenever brain is not a key therapeutic target (as MnTE-2-PyP^{5+} has low ability to cross blood brain barrier), MnTE-2-PyP^{5+} may be a superior candidate for clinical development. The main objective of the present study was to determine whether systemic administration of MnTE-2-PyP^{5+} would ameliorate radiation damage to the rectum and the development of acute and/or chronic radiation proctitis. This work is the first report on MnTE-2-PyP^{5+} radioprotection of GI tract where injuries occur when abdominal and pelvic regions are radiated.

Material and methods

All animal studies were reviewed and approved by the Loma Linda University Animal Care and Use Committee. A GMP batch of MnTE-2-PyP^{5+} was provided by National Jewish Health for this study.

Irradiation of the rectum

All irradiations were performed using male Sprague-Dawley rats weighing approximately 300 g. Animals were anesthetized with isoflurane for the duration of the irradiation procedure. After anesthesia induction, animals were secured to a fixation platform and then mounted on a positioning device with the 1.5 × 2.5 cm treatment beam entering the posterior (dorsal) surface. The position of the animal was then aligned using a light beam projected through the beam collimator and helium–neon alignment lasers. The long axis of the treatment beam was oriented in the rostral–caudal direction centered on midline with the caudal edge of the beam located 2.5 cm from the anus. In preliminary studies, field locations were identified using barium-contrasted CT and gadolinium-contrasted MRI, and confirmed with radiographs. A modulated, range-shifted proton beam was used to deliver the prescribed dose. Range shifting was used to position the shoulder of the treatment beam dose fall-off beyond the wall of the rectum, 2.5 cm into the body. 6 rats per group were studied. This setup was selected to ensure that all the animals received the prescribed dose over the full circumference of the rectum while minimizing the dose delivered to distal organs (bladder and ureter). A semiconductor dosimeter inserted into the rectum was used to confirm the dose delivered to the target. In all studies reported, a modulated proton beam was used to deliver the required dose to a 1.5 cm wide × 2.5 cm long × 2.5 cm deep rectal volume, 2.5 cm proximal to the anus. The 20–35 Gy protons were delivered to 2.5 cm span of rectum in male Sprague-Dawley rats using spread-out Bragg peak of a proton treatment beam. The relative biological effectiveness of the proton beam was taken to be 1.1, and all doses are reported as cobalt gray equivalents (CGE) [46]. Following the thinking of Van den Aardweg that the use of purgatives and metal insertions to localize the field altered the epithelial cell kinetics, it was decided not to utilize a purgative enema prior to irradiation [47].

The technique of "spreading out" the proton treatment beam is used both clinically and in the present study to ensure that a uniform dose is delivered over a range of depths, and to treat any target with axial dimension greater than few mm. The distal edge of the spread-out Bragg peak falls from 90% to 10% in few mm. To generate a uniform dose over a target at a greater range of depths than the Bragg Peak width the beam energy and intensity are moderated to generate successively shallower end of range beams. The full width at half maximum of the Bragg Peak for 200 MeV protons is about 2 cm; the maximum depth in tissue is about 25 cm. Single doses of protons for clinical cancer therapy range from 10 to 30 Gy, fractionated treatments from 10 to 15 Gy each and total absorbed dose up to 75 Gy.

Following radiation treatment, animals were removed from the fixation platform and fully recovered from anesthesia. Animals were then returned to the vivarium and maintained under standard care and diet with free access to food and water. All animals were observed daily by vivarium personnel, and weekly by one of the investigators until scheduled for sacrifice or removed from study due to the development of symptomatic chronic proctitis (changes in stool quality, mucosal or bloody discharge, weight loss, abdominal distension).

Preparation of specimens for histological studies

Following sacrifice, the anus, rectum, and a portion of the colon-rectum were exposed, measured *in situ*, then marked with permanent ink to indicate levels corresponding to the anus, and 2.5, 5, and 7 cm along the rectum. The terminal portions of the GI tract were then removed from the abdominal cavity and pinned to a Styrofoam flat so as to preserve the physical dimensions observed *in situ*. The levels from 2.0 cm to 6.5 cm were cut into sequential 5 mm blocks for fixation in 4% formaldehyde, and then embedded in paraffin. Sections from each block were cut at a thickness of 5 microns and stained with hematoxylin–eosin. The number of crypts on the rectal circumference was counted to assess the effect of proton irradiation and MnTE-2-PyP^{5+} treatment on the epithelial population (specimens derived from animals sacrificed 10–23 days post-irradiation). Rectal distension was assessed by measuring the area bounded by the rectal mucosa (cut in cross-section).

Statistics

All quantitative measures are reported as means $\pm$ standard error; group means were compared using the student *t*-test. A Log-Rank test was used to test the hypothesis that the time to development of chronic radiation proctitis was affected by SOD mimic administration. In all cases, statistical significance was assumed at $p < 0.05$.

Results

Radiation-based rectal injury

Acute phase

In evaluating the evolution of the acute proctitis, it was observed that the irradiated rats showed a characteristic sequence of radiation changes beginning with crypt loss and surface ulceration, which with time would be followed by crypt repopulation and regeneration (Fig. 2). This latter phase was largely completed by 23 days post-irradiation with 21.5 Gy. In the first phase we observed an initial shrinkage and collapse of the mucosal cellular architecture. Crypt mitoses decreased and stopped; cell outlines became indistinct; and then the cell was lost.

The deterioration was progressive, leading to crypt loss and surface denudation, which varied from moderate to severe in the irradiated animals (Fig. 3).

Radioprotective effects of MnTE-2-PyP^{5+}

Acute phase

Animals treated with the MnTE-2-PyP^{5+} administered (5 mg/kg, s.c.) either 1 h before or after irradiation, had a significantly greater number of crypts than untreated animals 10 days after irradiating the rectum with 21.5 Gy (Fig. 4). The smallest loss of crypts occurred in the pre-treated animals (61 ± 10% reduction in crypt density as compared to animals receiving no radiation). Animals which were given MnTE-2-PyP^{5+} as a post-treatment were observed to have a 73 ± 7% reduction in crypt density, while those receiving no treatment 92 ± 2%. MnTE-2-PyP^{5+} treatment had no significant effect on mucosal crypt density in animals receiving no radiation.

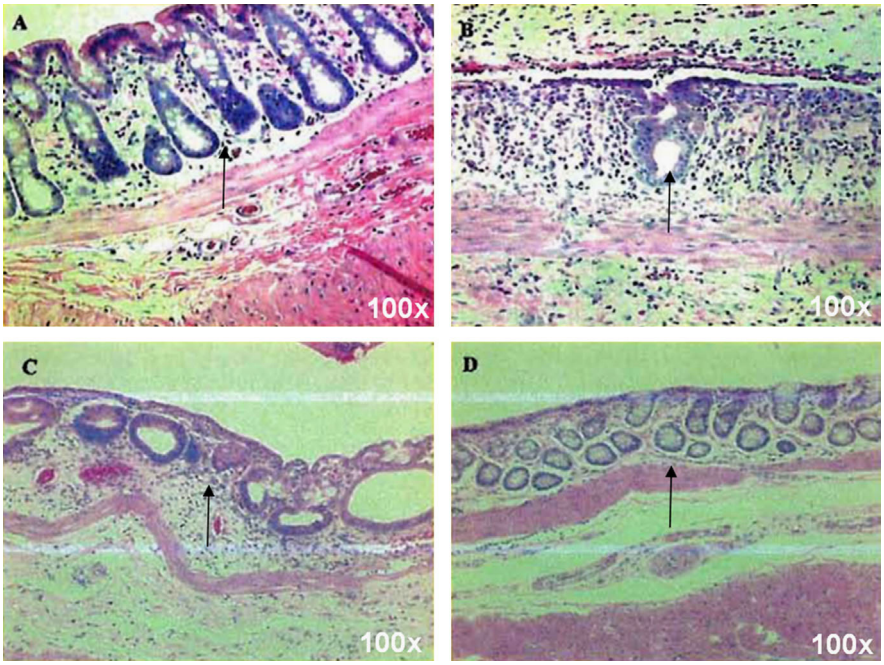

Fig. 2. The acute temporal effects of radiation therapy upon rectal mucosa. Temporal changes in the rectal mucosa following irradiation with 21.5 Gy from 10 to 16 and 23 days after radiation; Panel A. Control mucosa from an unirradiated rat; Panel B. 10 days post-irradiation. Ulcerated surface of the mucosa with a single surviving crypt on the opposing surface; Panel C. Repopulating crypts observed 16 days post irradiation; Panel D. Repopulated crypts 23 days following irradiation. The H&E staining was done at 100-fold magnification. 6 rats per group were studied.

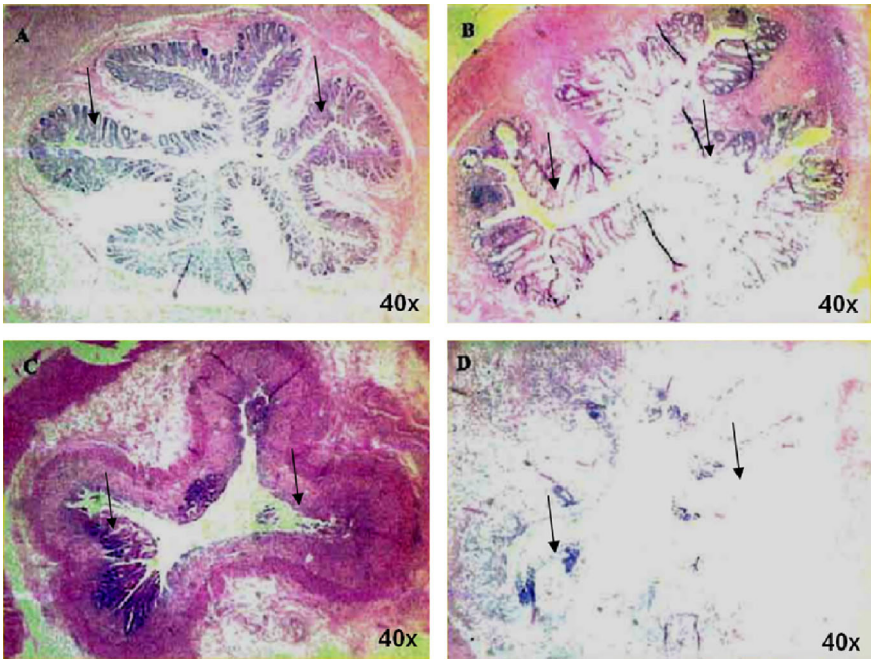

Fig. 3. The variability of the acute effects of radiation upon rectal mucosa. Acute radiation effects on the rectal mucosa, 10 days following irradiation with 21.5 CGE. The continuous mucosa observed in normal rectal tissue (Panel A) was markedly disrupted in all the irradiated animals studied. The severity of this effect was variable as demonstrated in panels B, C and D, representative of moderate, severe and near total loss of the rectal mucosal lining. The magnitude of crypt loss observed at 10 days post irradiation was reduced by both pre-treatment and post-treatment with systemically administered MnTE-2-PyP^{5+} as shown in Fig. 4. The H&E staining was done at 40-fold magnification. 6 rats per group were studied.

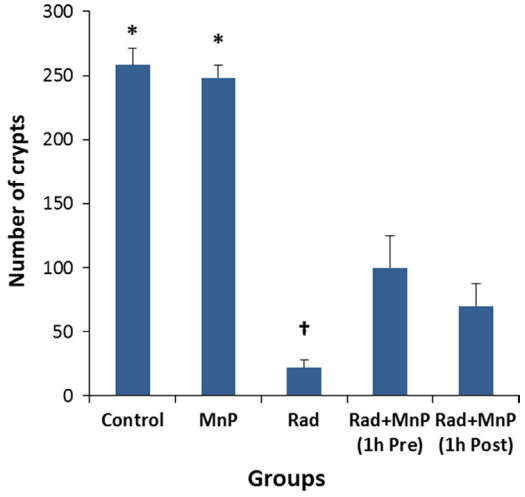

Fig. 4. Acute protective effects of MnTE-2-PyP^{5+} (MnP) on the radiation-based loss of crypts. Control group of rats received no radiation and no MnP administration. MnP group received no radiation, only MnP administration. Rad group received radiation and no MnP treatment. The surviving number of crypts is presented facing the basement membrane on the circumference of the rectum in animals euthanized at 10 days after focal irradiation of a 2.5 cm segment of the rectum with single fraction of 21.5 Gy. Rad+MnP groups: Pre-treatment dosage: MnTE-2-Py^{5+} (5 mg/kg s.c.) administered 1 h before irradiation and 7 days post-irradiation. Post-treatment dosage: MnTE-2-PyP^{5+} (5 mg/kg s.c.) administered 1 h and 7 days post-irradiation. *Significantly higher than other groups ($p<0.05$); † Significantly lower than other groups ($p<0.05$). 6 rats per group were studied.

Chronic phase

Two chronic studies were performed. In the first, all animals (6 per group) were randomized into one of the three treatment regimens prior to irradiation with 21.5 Gy: Group with no MnTE-2-PyP^{5+} treatment; Group with Pre-treatment (MnTE-2-PyP^{5+}, 5 mg/kg subcutaneous, administered 1 h prior to irradiation and at weekly intervals thereafter); and group with Post-treatment (with the initial dose of MnTE-2-PyP^{5+}, 5 mg/kg s.c., given 1 h after irradiation).

Animals receiving MnTE-2-PyP^{5+} 1 h prior to irradiation showed no untoward signs or symptoms, and remained active throughout the subsequent 150 days of observation. Animals showed normal weight gain throughout the post-irradiation interval. Gross and histological examination revealed no abnormal findings.

In the group given MnTE-2-PyP^{5+} 1 h post irradiation, 4 of the 6 animals became moribund prematurely and were removed from study; 2 out of these 4 had rectal dilation and diarrhea, and 2 more displayed intensive inflammatory infiltrates with mucosal ulceration and denuded mucosal surfaces typical of the histological changes described by Trott. The two surviving animals continued to receive MnTE-2-PyP^{5+} injections for the remaining weeks of observation. These surviving animals showed normal weight gain. At necropsy on day 150, diarrhea and a dilated rectum were noted. At biopsy, the mucosa was intact although the lumen was markedly dilated (Fig. 5). The mucosa was re-epitheliated and hyperplastic. Similar findings were noted in the untreated, irradiated animals.

Rectal dilation in these animals was quantified at the time of necropsy. The average areas of the rectal lumen for the untreated and post-treated irradiated animals were 57.1 ± 5.1 mm^2 and 57.2 ± 4.1 mm^2. In both cases, the measured areas were significantly greater than those observed in control (non-irradiated) cohorts (17.4 ± 2.4 mm^2) or in pre-treated animals (15.9 ± 1.5 mm^2).

In a second series, we examined the effects of the MnTE-2-PyP^{5+} pre-treatment and radiation dose on the time to development of clinical signs of chronic proctitis (diarrhea, mucosal or bloody discharge, weight loss, abdominal distension). As expected, the time to onset of chronic proctitis was radiation dose dependent, with higher doses associated with earlier onset of clinical signs. MnTE-2-PyP^{5+} treatment significantly delayed or prevented the development of chronic proctitis at the lower radiation doses examined (20, 25, and 30 Gy). The protective effects of treatment were not observed in animals irradiated with the 35 Gy dose. These findings are summarized in Fig. 6.

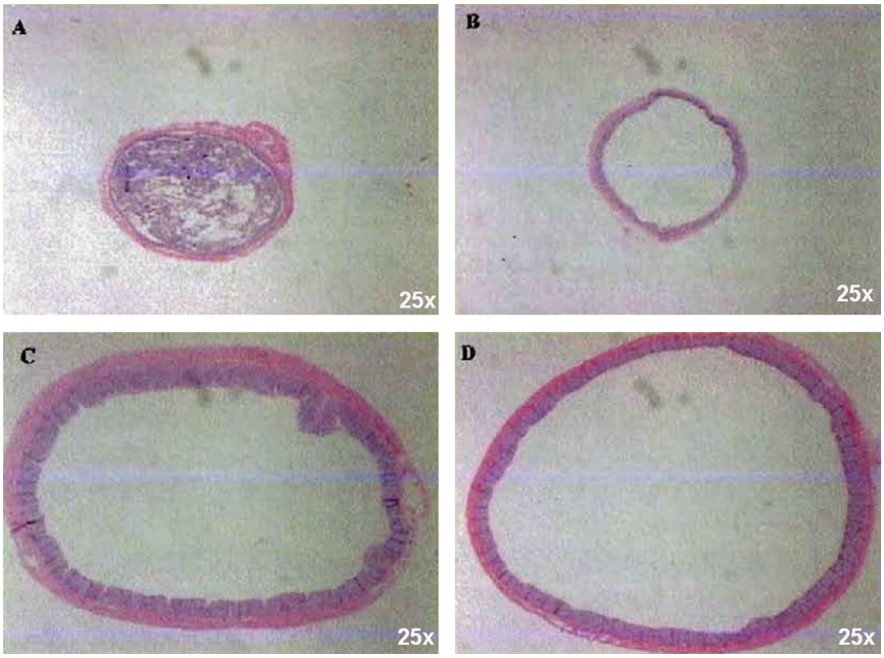

Fig. 5. The chronic effects of radiation and the efficacy of MnTE-2-PyP^{5+} in suppressing rectal dilation. Photomicrographs of rectal cross-sections were taken at 150 days post-irradiation, demonstrating rectal dilation and the effects of MnTE-2-PyP^{5+} treatment. Panel A relates to unirradiated control group. Typical specimen obtained from animals receiving MnTE-2-PyP^{5+} 1 h prior to receiving 21.5 Gy protons (Panel B) and MnTE-2-PyP^{5+} 1 h after receiving 21.5 Gy protons (Panel C). Panel D: Specimen taken from animal receiving 21.5 Gy protons without MnTE-2-PyP^{5+} treatment. Note the hyperplastic mucosa in Panels C and D which was a typical finding in both treatment groups. The H&E staining is shown at 25-fold magnification. 6 rats per group were studied.

None of the animals developed hydronephrosis during the 225 days following irradiation, the termination point for the second chronic series. Histological examination performed after necropsy showed characteristic signs of chronic proctitis, including mucosal atrophy, inflammation, submucosal fibrosis and vasculopathy.

Discussion

Following a single dose fraction of 21.5 Gy, an acute proctitis was produced. The response was ameliorated by MnTE-2-PyP^{5+} administration. The number of crypts in the group receiving MnTE-2-PyP^{5+} 1 h prior to irradiation was larger by a factor of five than the group given proton irradiation and no MnTE-2-PyP^{5+}. All irradiated groups survived the acute proctitis period. This indicates that the surviving cell fractions were able to replace the cells lost. The time elapsed between the acute proctitis and onset of diarrhea and rectal dilation in the present study overlapped the proctitis described by others. Since we did not wish to duplicate previous efforts to define the ED50 for development of chronic proctitis at 150 days, 21.5 Gy was used as the target dose and 150 days as the time lapse to euthanize the survivors based on findings reported by Hubmann [12]. A noteworthy observation in the present study was the uniform gross changes of dilation seen in untreated and post-treated, irradiated animals under these conditions. Tamou and Trott also observed stretching of the rectum and a progressive distensibility up to the 29th week post-irradiation [48]. These observations do not preclude that the other late effects were evolving and so reflect a period of chronic proctitis. We consider our own observations consistent with Trott's definitions of chronic proctitis.

The uniform dilation of the rectum at 150 days seen in this work was consistent with earlier findings and conclusions of van den Aadweg, suggesting that dilation may precede inflammatory changes, mucosal atrophy, and scarring [47]. Moribund rats removed from the present study for humane reasons presented with the rectal changes noted by Trott, and all untreated and post-treated rats surviving to 150 days presented with rectal dilation and diarrhea. This sequence implies continuity between our own and previous histologic studies and suggests that if the observations had continued longer than 5 months the mucosal atrophy, inflammation, and scarring phases described by Trott might have appeared. This was confirmed in our second chronic series. Another difference existing between the present and earlier studies results from an expectation that a point of stricture exists between the dilated rectum and the irradiated rectum. We found no evidence for the formation of a fibrotic stricture in any of the animals studied. A suggested explanation was that a pseudo stricture point resulted from muscular atony produced by irradiation. These different histological results reflect, presumably, the difference in the selected protocol conditions. We utilized a 1.5-cm-wide proton beam of fixed length (2.5 cm) to irradiate male Sprague-Dawley rats. Trott's group used a 1.0-cm wide beam of lengths that varied up to 5 cm long, a spread of single dose fractions using 300 kV X rays and female Wistar rats. It is well to recall that there are reported differences in biological response between X-ray and protons [49].

Breiter and Trott showed that following a fractionated time–dose schedule of 6, 7, or 8 Gy delivered at 10-day intervals over a period of 170 days (18 dose fractions in 170 days), an acute proctitis did not occur. Late proctitis did occur over the ensuing 160 days [17]. This suggests that the casual elements were delayed but connected (masked). Similarly, animals fed a low-fiber diet did not develop an acute proctitis, but when the original diet was restarted a chronic proctitis with intestinal obstruction appeared after a period of a week [50]. This observation also documents the importance of the fecal pellets as a necessary causal element and indicates an additional latent period.

Another example suggesting a variable latent period was that the irradiation of 18 rats with a 10×10 mm field did not produce signs of an acute proctitis or, later, a chronic proctitis. However, when a 35 mm $\times$ 10 field was superimposed over the smaller

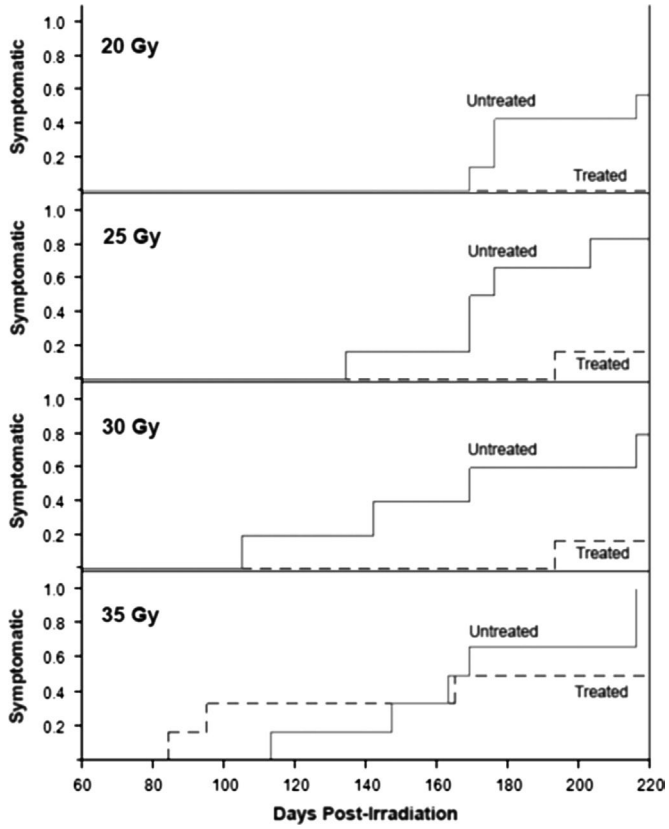

Fig. 6. The fraction of rats developing radiation proctitis is dependent upon the dose of radiation and MnTE-2-PyP^{5+} treatment. Kaplan–Meier plots showing the effects of radiation dose and MnTE-2-PyP^{5+} treatment on the time to onset of symptoms of chronic proctitis in irradiated rats. For each dose, the fraction of animals entered into study which exhibited symptoms of chronic proctitis are shown for days 60 through 225. MnTE-2-PyP^{5+} treatment (weekly subcutaneous administration of 5 mg/kg beginning 1 h before irradiation) delayed or prevented the development of symptoms of chronic proctitis, an effect which dependent on the radiation dose delivered. No beneficial effects of MnTE-2-PyP^{5+} treatment were observed at the highest radiation dose tested. 6 rats per group were studied.

irradiation area, a chronic proctitis appeared. Eleven ulcers extended throughout the boost field, while 7 were limited to the original small field, with a latency of 350 days post irradiation. Involvement of the larger field had an average latency of 300 days following the boost [9]. The chronic ulceration and histological changes in these rats were identical to the changes produced by single-dose fractions with a shorter latency of 115 days. Black et al. irradiated the rectum with a single dose fraction to deliver a total dose of 20–50 Gy, and 60–100 Gy using five or ten fractions. Mucosal changes consisted of ulceration, colitis, cystica profunda, atypical epithelial regeneration, fibrosis, or vascular sclerosis in non-capillary vessels. All of these abnormalities were observed in the present study at the higher dose range examined. Severe lesions included chronic deep ulcers, fistulae, and high-grade strictures. Ulceration did not occur as an isolated lesion [14]. None of these lesions were detected in the present series.

Clinical relevance of rat study

In clinical settings, normal tissue complication probability (NTCP), for example the risk of developing proctitis following pelvic RT, determines dose delivered to the treatment target – the tumor. In the present study, a dose range was studied that would encompass the NTCP encountered clinically. In that sense, the doses are clinically relevant. However, the radiosensitivity of the GI epithelium depends in part on the volume of tissue irradiated. Indeed, had the 20–30 Gy dose been delivered to the whole body, or even the entire gut, none of those animals would survive. Nor would a single fraction, 20–30 Gy dose of proton or X-radiation be used in radiation treatment (RT) outside of radiosurgical applications (in which a toxic dose of radiation is intentionally delivered to a target). As a general rule, the smaller the volume of the tissue, the less radiosensitive the tissue is. Rodent models of RT-related radiotoxicity require greater total dose than would be used clinically to produce a toxicity endpoint of interest such as GI epithelial damage. However, in rodent radiotoxicity studies the relatively small volumes of irradiated tissue involved necessitates, increasing the effective dose beyond that which would be used clinically to produce the desired endpoint for study, *i.e.* proctitis. This is a significant source of uncertainty in extrapolating from rodent models to humans. Thus, the question is whether the mechanism by which the single fraction radiation dose delivered to rats damages the GI epithelial and triggers symptoms of proctitis is the same as the mechanism which occurs with fractionated treatment doses used clinically. This issue would have to be resolved in follow up studies in which various degrees of hypofractionation are studied.

Therapeutic vs. cytotoxic effects of Mn porphyrin-based SOD mimics

The radiation dose-dependent data obtained in the range of 20–35 Gy prove that the magnitude of oxidative stress has large impact on the type and magnitude of the outcome. MnTE-2-PyP^{5+} was radioprotective up to 30 Gy, but not at 35 Gy (Fig. 7). Moreover it increased the number of rats with proctitis, thus enhancing radiation damage. Until recently we would not have understand such opposing effects. The master transcription factor, NF-κB plays a major role in the actions of Mn porphyrins. Our data collected thus far taught us that the action of Mn porphyrins upon inhibition of this antiapoptotic prosurvival transcription factor occurs *via* oxidation of cysteines of NF-κB subunits p50 and p65 in the presence of GSH and H_2O_2 which prevents its DNA binding and in turn its transcriptional activity [21,26]. Subsequent comprehensive aqueous chemistry and biology studies [21,25,51] support a major role of H_2O_2 in the actions of Mn porphyrins. At low levels of H_2O_2, the limited inhibition of NF-κB DNA binding would suppress excessive inflammation, while at high levels of H_2O_2 the major

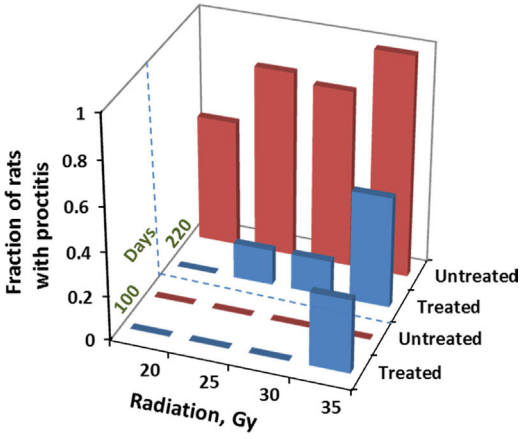

Fig. 7. Schematic presentation of the dependence of shift of anti- (therapeutic) to pro-oxidative (cytotoxic) outcome of Mn porphyrin-based therapy upon the magnitude of oxidative stress as a consequence of the magnitude of radiation. The data relate to 100 and 220 days after radiation. Blue bars indicate results from MnP-treated rats, while red bars relate to radiation-only treated rats. The fraction of rats which developed radiation proctitis is given on *Y*-axis. In the range of 20–30 Gy MnTE-2-PyP^{5+} is radioprotective, reducing the fraction of rats with proctitis. At radiation doses above 30 Gy, Mn porphyrin amplified the cytotoxic effects of radiation. (For interpretation of the references to color in this figure legend, the reader is referred to the web version of this article.)

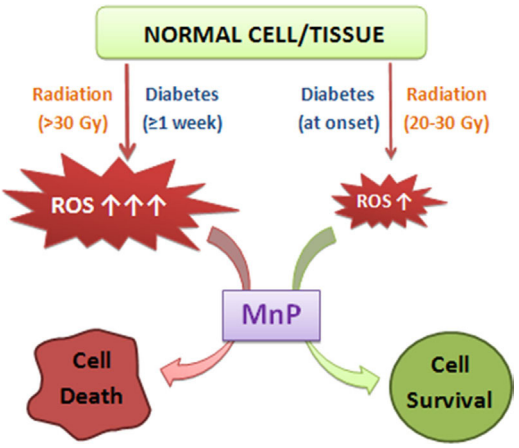

Fig. 8. The schematic presentation of the opposing *in vivo* effects of Mn porphyrin (therapeutic *vs.* cytotoxic) as substantiated in this study and in diabetes study. When MnTE-2-PyP^{5+} is given at a time point when the oxidative stress is not overwhelming and cell has not yet initiated death, the MnP produces therapeutic (antioxidative) effects. However, when the oxidative damage has already escalated and levels of reactive species are largely increased relative to normal or mildly sick cell/organism, MnP enhances the damage. MnP produces H_2O_2 by reducing oxygen to superoxide and superoxide to H_2O_2. Under physiological conditions, H_2O_2 is taken care of by abundant and redundant endogenous peroxide-removing enzymes such as families of catalases, glutathione peroxidases, peroxyredoxins, thioredoxins etc. However, under pathological conditions some of thiol-based enzymes may be heavily oxidized and/or downregulated. Thus, MnP will frequently encounter H_2O_2, and will employ it to catalyze the oxidation of such targets as simple and protein thiols, NADH and NADPH, lipids etc [3,8, Tovmasyan et al. FRBM Supplement 2, 2013]. Consequently, under pathological conditions of excessive oxidative stress (as is too high radiation dose or advanced diabetes), MnP could amplify the damage and promote cell death. Please see Refs. [21,26] for the impact of MnP in production of H_2O_2 and utilization of H_2O_2 to oxidize biological molecules.

suppression of NF-κB would result in apoptosis and eventually cell death. Such shift in the nature of effects produced by MnTE-2-PyP^{5+} is schematically presented in Figs. 7 and 8. At day 100 after 35 Gy radiation, no chronic proctitis was found with MnTE-2-PyP^{5+}-non-treated rats, but ~40% rats have proctitis in MnTE-2-PyP^{5+}-treated group. Similar cytotoxic effect of MnP was observed at day 220 after 35 Gy radiation.

We have recently demonstrated a similar scenario in a diabetes study. The methyl analog, MnTM-2-PyP^{5+}, reduced kidney damage in a sreptozotocin rat model of diabetes when its administration started at the onset of diabetes (24 h after STZ injection) [26]. Yet, when Mn porphyrin therapy started 8 days after the onset of diabetes, the cytotoxic effects, *i.e.* the enhancement of kidney damage has been observed [26]. We have depicted such opposite effects of MnP in diabetes and rectum radioprotection study in Fig. 8.

Such differential effects – cytoprotective if the disease has not advanced beyond certain threshold and cytotoxic if oxidative stress is ragging – is presently explored with cancer radiation therapy to our advantage in killing tumor (tissue of excessive oxidative stress), but healing the normal tissue.

Finally, in several other studies, when Mn porphyrin has been administered with excessive amounts of ascorbate (H_2O_2 producing system), only the cytotoxic action has been observed [52–56]. Such system is in development for tumor treatment with us and others. Further studies are in progress to clarify the role of Mn porphyrins and reductants in healing the normal tissue, yet killing the cancer cell.

Conclusions

Rectal proctitis is a severe clinical problem that occurs at acute and chronical level as a consequence of abdominal and pelvic radiations. MnTE-2-PyP^{5+} proved efficacious in protecting lower part of colon from radiation. All rats survived the acute proctitis following irradiation of the 2.5 cm rectal segment with up to 35 Gy. This indicates that a sufficient fraction of epithelial cells survived and were capable of re-populating the mucosa. The administration of MnTE-2-PyP^{5+} either immediately before or after irradiation protects against radiation induced crypt loss. When MnTE-2-PyP^{5+} was administered 1 h before proton irradiation (21.5 Gy), it protected against the development of delayed rectal dilation, mucosal changes, or diarrhea. However none of those effects were observed if MnTE-2-PyP^{5+} was administered 1 h after radiation. The pretreatment with MnTE-2-PyP^{5+}, with weekly MnP administration and radiation dose of up to 30 Gy after, delayed the development of chronic proctitis. Significantly protective effects are produced with 21.5 Gy, which is far away from the dose (~35 Gy) where MnP enhanced the radiation toxicity.

The nature and the magnitude of the effects of MnTE-2-PyP^{5+}-based radiation therapy largely depend upon the magnitude of the oxidative stress produced by radiation: at lower radiation doses MnTE-2-PyP^{5+} is radioprotective, but enhances radiation damage at higher radiation doses. Under latter conditions it presumably (based on the correlation of the results of this and earlier studies) employs excessive oxidative stress, produced by high radiation dose, more specifically the H_2O_2, to catalyze the vast oxidation of pro-survival proteins/transcription factors and simple molecules essential for supplying the reducing equivalent for metabolic processes.

MnTE-2-PyP^{5+} and the related low molecular-weight cationic *N*-substituted pyridyl- and *N,N'*-disubstituted imidazolylporphyrin-based SOD mimics, who exhibit the ability to normalize the cellular redox environment and promote survival, warrant further investigation as adjunctive treatment along with radiotherapy of tumors located in the abdominal and pelvic regions.

Acknowledgments

The authors wish to thank Nathan Lindsey and Stephen Rightnar for their expert technical assistance. The drug MnTE-2-PyP^{5+} was kindly donated by National Jewish Health. Artak Tovmasyan and Ines Batinic-Haberle acknowledge General Research Funds of Ines Batinic-Haberle.

References

[1] A.K. Shadad, F.J. Sullivan, J.D. Martin, L.J. Egan, Gastrointestinal radiation injury: prevention and treatment, World J. Gastroenterol. 19 (2013) 199–208.
[2] M. Hauer-Jensen, J. Wang, M. Boerma, Q. Fu, J.W. Denham, Radiation damage to the gastrointestinal tract: mechanisms, diagnosis, and management, Curr. Opin. Support Palliat. Care 1 (2007) 23–29.
[3] C. Henson, Chronic radiation proctitis: issues surrounding delayed bowel dysfunction post-pelvic radiotherapy and an update on medical treatment, Ther. Adv. Gastroenterol. 3 (2010) 359–365.
[4] M.L. Rodriguez, M.M. Martin, L.C. Padellano, A.M. Palomo, Y.I. Puebla, Gastrointestinal toxicity associated to radiation therapy, Clin. Transl. Oncol. 12 (2010) 554–561.
[5] A.K. Shadad, F.J. Sullivan, J.D. Martin, L.J. Egan, Gastrointestinal radiation injury: symptoms, risk factors and mechanisms, World J. Gastroenterol. 19 (2013) 185–198.
[6] M.T. Wong, J.F. Lim, K.S. Ho, B.S. Ooi, C.L. Tang, K.W. Eu, Radiation proctitis: a decade's experience, Singap. Med. J. 51 (2010) 315–319.
[7] R.R. Babb, Radiation proctitis: a review, Am. J. Gastroenterol. 91 (1996) 1309–1311.
[8] J.M. Michalski, H. Gay, A. Jackson, S.L. Tucker, J.O. Deasy, Radiation dose-volume effects in radiation-induced rectal injury, Int. J. Radiat. Oncol. Biol. Phys. 76 (2010) S123–S129.
[9] K.R. Trott, Chronic damage after radiation therapy: challenge to radiation biology, Int. J. Radiat. Oncol. Biol. Phys. 10 (1984) 907–913.
[10] Z. Kiszel, A. Spiethoff, K.R. Trott, Large bowel stenosis in rats after fractionated local irradiation, Radiother. Oncol. 2 (1984) 247–254.

[11] N. Breiter, P. Kneschaurek, G. Burger, J. Huczkowski, K.R. Trott, The r.b.e. of fast fission neutrons (2 MeV) for chronic radiation damage of the large bowel of rats after single dose and fractionated irradiation, Int. J. Radiat. Biol. Relat. Stud. Phys. Chem. Med. 49 (1986) 1031–1038.

[12] F.H. Hubmann, Effect of X irradiation on the rectum of the rat, Br. J. Radiol. 54 (1981) 250–254.

[13] M.G. Northway, M.W. Scobey, K.R. Geisinger, Radiation proctitis in the rat. Sequential changes and effects of anti-inflammatory agents, Cancer 62 (1988) 1962–1969.

[14] W.C. Black, L.S. Gomez, J.M. Yuhas, M.M. Kligerman, Quantitation of the late effects of X-radiation on the large intestine, Cancer 45 (1980) 444–451.

[15] L. Lundby, J. Overgaard, S. Laurberg, Histopathological and morphometric analyses of late rectal injury after irradiation, APMIS 108 (2000) 216–222.

[16] K.R. Trott, S. Tamou, T. Sassy, Z. Kiszel, The effect of irradiated volume on the chronic radiation damage of the rat large bowel, Strahlenther. Onkol. 171 (1995) 326–331.

[17] N. Breiter, K.R. Trott, Chronic radiation damage in the rectum of the rat after protracted fractionated irradiation, Radiother. Oncol. 7 (1986) 155–163.

[18] J.F. Knowles, K.R. Trott, Experimental irradiation of the rat ureter: the effects of field size and the presence of contrast medium on incidence and latency of hydronephrosis, Radiother. Oncol. 10 (1987) 59–66.

[19] I. Batinic-Haberle, J.S. Reboucas, I. Spasojevic, Superoxide dismutase mimics: chemistry, pharmacology, and therapeutic potential, Antioxid. Redox Signal 13 (2010) 877–918.

[20] I. Batinic-Haberle, I. Spasojevic, H.M. Tse, A. Tovmasyan, Z. Rajic St, D.K. Clair, Z. Vujaskovic, M.W. Dewhirst, J.D. Piganelli, Design of Mn porphyrins for treating oxidative stress injuries and their redox-based regulation of cellular transcriptional activities, Amino Acids 42 (2012) 95–113.

[21] I. Batinic-Haberle, A. Tovmasyan, E. Roberts, Z. Vujaskovic, K.W. Leong, I. Spasojevic, SOD therapeutics: latest insights into their structure–activity relationships and impact upon the cellular redox-based pathways, Antioxid. Redox Signal, 10.1089.ars.2012.5147, in press.

[22] A. Tovmasyan, H. Sheng, T. Weitner, A. Arulpragasam, M. Lu, D.S. Warner, Z. Vujaskovic, I. Spasojevic, I. Batinic-Haberle, Design, mechanism of action, bioavailability and therapeutic effects of Mn porphyrin-based redox modulators, Med. Princ. Pract. 22 (2013) 103–130.

[23] I. Batinić-Haberle, I. Spasojević, P. Hambright, L. Benov, A.L. Crumbliss, I. Fridovich, Relationship among redox potentials, proton dissociation constants of pyrrolic nitrogens, and in vivo and in vitro superoxide dismutating activities of manganese(iii) and iron(iii) water-soluble porphyrins, Inorg. Chem. 38 (1999) 4011–4022.

[24] J.S. Reboucas, G. DeFreitas-Silva, I. Spasojevic, Y.M. Idemori, L. Benov, I. Batinic-Haberle, Impact of electrostatics in redox modulation of oxidative stress by Mn porphyrins: protection of SOD-deficient *Escherichia coli* via alternative mechanism where Mn porphyrin acts as a Mn carrier, Free Radic. Biol. Med. 45 (2008) 201–210.

[25] A. Tovmasyan, T. Weitner, E. Roberts, M. Jaramillo, I. Spasojevic, K. Leong, M. Tome, L. Benov, I. Batinic-Haberle, Understanding differences in mechanisms of action of Fe vs. Mn porphyrins: comparison of their reactivities towards cellular reductants and reactive species, Free Radic. Biol. Med. 53 (2012) S120.

[26] D. Ali, M. Oriowo, A. Tovmasyan, I. Batinic-Haberle, L. Benov, Late administration of Mn porphyrin-based SOD mimic enhances diabetic complications, Redox Biol. 1 (2013) 457–466.

[27] M.C. Jaramillo, M.M. Briehl, I. Batinic-Haberle, M.E. Tome, Inhibition of the electron transport chain via the pro-oxidative activity of manganese porphyrin-based SOD mimetics modulates bioenergetics and enhances the response to chemotherapy, Free Radic. Biol. Med. 65 (2013) S30.

[28] I. Batinic-Haberle, J.S. Reboucas, L. Benov, I. Spasojevic, Chemistry, biology and medical effects of water soluble metalloporphyrins, in: K.M. Kadish, K. M. Smith, R. Guillard (Eds.), Handbook of Porphyrin Science, World Scientific, Singapore, 2011, pp. 291–393.

[29] B. Gauter-Fleckenstein, K. Fleckenstein, K. Owzar, C. Jiang, I. Batinic-Haberle, Z. Vujaskovic, Comparison of two Mn porphyrin-based mimics of superoxide dismutase in pulmonary radioprotection, Free Radic. Biol. Med. 44 (2008) 982–989.

[30] B. Gauter-Fleckenstein, K. Fleckenstein, K. Owzar, C. Jiang, J.S. Reboucas, I. Batinic-Haberle, Z. Vujaskovic, Early and late administration of MnTE-2-PyP^{5+} in mitigation and treatment of radiation-induced lung damage, Free Radic. Biol. Med. 48 (2010) 1034–1043.

[31] D.S. Gridley, A.Y. Makinde, X. Luo, A. Rizvi, J.D. Crapo, M.W. Dewhirst, B.J. Moeller, R.D. Pearlstein, J.M. Slater, Radiation and a metalloporphyrin radioprotectant in a mouse prostate tumor model, Anticancer Res. 27 (2007) 3101–3109.

[32] A.Y. Makinde, A. Rizvi, J.D. Crapo, R.D. Pearlstein, J.M. Slater, D.S. Gridley, A metalloporphyrin antioxidant alters cytokine responses after irradiation in a prostate tumor model, Radiat. Res. 173 (2010) 441–452.

[33] S. Mehrotra, M.J. Pecaut, T.L. Freeman, J.D. Crapo, A. Rizvi, X. Luo-Owen, J.M. Slater, D.S. Gridley, Analysis of a metalloporphyrin antioxidant mimetic (MnTE-2-PyP) as a radiomitigator: prostate tumor and immune status, Technol. Cancer Res. Treat. 11 (2012) 447–457.

[34] J.H. Lee, Y.M. Lee, J.W. Park, Regulation of ionizing radiation-induced apoptosis by a manganese porphyrin complex, Biochem. Biophys. Res. Commun. 334 (2005) 298–305.

[35] J.H. Lee, J.W. Park, A manganese porphyrin complex is a novel radiation protector, Free Radic. Biol. Med. 37 (2004) 272–283.

[36] X.W. Mao, J.D. Crapo, T. Mekonnen, N. Lindsey, P. Martinez, D.S. Gridley, J.M. Slater, Radioprotective effect of a metalloporphyrin compound in rat eye model, Curr. Eye Res. 34 (2009) 62–72.

[37] R.D. Pearlstein, Y. Higuchi, M. Moldovan, K. Johnson, S. Fukuda, D.S. Gridley, J.D. Crapo, D.S. Warner, J.M. Slater, Metalloporphyrin antioxidants ameliorate normal tissue radiation damage in rat brain, Int. J. Radiat. Biol. 86 (2010) 145–163.

[38] Z. Vujaskovic, I. Batinic-Haberle, Z.N. Rabbani, Q.F. Feng, S.K. Kang, I. Spasojevic, T.V. Samulski, I. Fridovich, M.W. Dewhirst, M.S. Anscher, A small molecular weight catalytic metalloporphyrin antioxidant with superoxide dismutase (SOD) mimetic properties protects lungs from radiation-induced injury, Free Radic. Biol. Med. 33 (2002) 857–863.

[39] R.E. Oberley-Deegan, J.J. Steffan, K.O. Rove, K.M. Pate, M.W. Weaver, I. Spasojevic, B. Frederick, D. Raben, R.B. Meacham, J.D. Crapo, H.K. Koul, The antioxidant, MnTE-2-PyP, prevents side-effects incurred by prostate cancer irradiation, PLoS One 7 (2012) e44178.

[40] Y. Zhang, X. Zhang, Z.N. Rabbani, I.L. Jackson, Z. Vujaskovic, Oxidative stress mediates radiation lung injury by inducing apoptosis, Int. J. Radiat. Oncol. Biol. Phys. 83 (2012) 740–748.

[41] Weitzel D., A.K., Liu C., Li W., Buckley A., Rodriguiz R.M., Wetsel W.C., Spasojevic I., Tovmasyan A., Peters K.B., Batinic-Haberle I., Dewhirst MW. Radioprotection of brain white matter by the catalytic MnSOD mimic/antioxidant, BMX-001. Pediatric Neuro-Oncology Basic and Translational Research Conference, Ft. Lauderdale, Florida, 2013.

[42] S. Miriyala, I. Spasojevic, A. Tovmasyan, D. Salvemini, Z. Vujaskovic St, D. Clair, I. Batinic-Haberle, Manganese superoxide dismutase, MnSOD and its mimics, Biochim. Biophys. Acta 1822 (2012) 794–814.

[43] I. Spasojevic, Y. Chen, T.J. Noel, Y. Yu, M.P. Cole, L. Zhang, Y. Zhao St, D.K. Clair, I. Batinic-Haberle, Mn porphyrin-based superoxide dismutase (SOD) mimic, Mn^{III}TE-2-PyP^{5+}, targets mouse heart mitochondria, Free Radic. Biol. Med. 42 (2007) 1193–1200.

[44] M.M. Delmastro-Greenwood, T. Votyakova, E. Goetzman, M.L. Marre, D.M. Previte, A. Tovmasyan, I. Batinic-Haberle, M. Trucco, J.D. Piganelli, Mn porphyrin regulation of aerobic glycolysis: implications on the activation of diabetogenic immune cells, Antioxid. Redox. Signal, 10.1089/ars.2012.5167.

[45] H. Sheng, R.E. Chaparro, T. Sasaki, M. Izutsu, R.D. Pearlstein, A. Tovmasyan, D.S. Warner, Metalloporphyrins as therapeutic catalytic oxidoreductants in central nervous system disorders, Antioxid. Redox Signal (2013).

[46] H. Paganetti, A. Niemierko, M. Ancukiewicz, L.E. Gerweck, M. Goitein, J.S. Loeffler, H.D. Suit, Relative biological effectiveness (RBE) values for proton beam therapy, Int. J. Radiat. Oncol. Biol. Phys. 53 (2002) 407–421.

[47] G.J. van den Aardweg, M.J. Olofsen-van Acht, C.M. van Hooije, P.C. Levendag, Radiation-induced rectal complications are not influenced by age: a dose fractionation study in the rat, Radiat. Res. 159 (2003) 642–650.

[48] S. Tamou, K.R. Trott, The effects of local X-irradiation on the distensibility of the rectum in rats, Br. J. Radiol. 68 (1995) 64–69.

[49] D.S. Gridley, R.B. Bonnet, D.A. Bush, C. Franke, G.A. Cheek, J.D. Slater, J.M. Slater, Time course of serum cytokines in patients receiving proton or combined photon/proton beam radiation for resectable but medically inoperable non-small-cell lung cancer, Int. J. Radiat. Oncol. Biol. Phys. 60 (2004) 759–766.

[50] N. Breiter, K.R. Trott, The pathogenesis of the chronic radiation ulcer of the large bowel in rats, Br. J. Cancer Suppl. 7 (1986) 29–30.

[51] A. Tovmasyan, T. Weitner, H. Sheng, M. Lu, Z. Rajic, D.S. Warner, I. Spasojevic, J.S. Reboucas, L. Benov, I. Batinic-Haberle, Differential coordination demands in Fe versus Mn water-soluble cationic metalloporphyrins translate into remarkably different aqueous redox chemistry and biology, Inorg. Chem. 52 (2013) 5677–5691.

[52] I. Batinic-Haberle, Z. Rajic, L. Benov, A combination of two antioxidants (an SOD mimic and ascorbate) produces a pro-oxidative effect forcing *Escherichia coli* to adapt via induction of oxyR regulon, Anticancer Agents Med. Chem. 11 (2011) 329–340.

[53] M.K. Evans, A. Tovmasyan, I. Batinic-Haberle, G.R. Devi, Mn porphyrin in combination with ascorbate acts as a pro-oxidant and mediates caspase-independent cancer cell death, Free Radic. Biol. Med. (2013)(in preparation).

[54] M. Rawal, S.R. Schroeder, B.A. Wagner, C.M. Cushing, J.L. Welsh, A.M. Button, J. Du, Z.A. Sibenaller, G.R. Buettner, J.J. Cullen, Manganoporphyrins increase ascorbate-induced cytotoxicity by enhancing H_2O_2 generation, Cancer Res. 73 (2013) 5232–5241.

[55] J. Tian, D.M. Peehl, S.J. Knox, Metalloporphyrin synergizes with ascorbic acid to inhibit cancer cell growth through fenton chemistry, Cancer Biother. Radiopharm. 25 (2010) 439–448.

[56] X. Ye, D. Fels, A. Tovmasyan, K.M. Aird, C. Dedeugd, J.L. Allensworth, I. Kos, W. Park, I. Spasojevic, G.R. Devi, M.W. Dewhirst, K.W. Leong, I. Batinic-Haberle, Cytotoxic effects of Mn(III) N-alkylpyridylporphyrins in the presence of cellular reductant, ascorbate, Free Radic. Res. 45 (2011) 1289–1306.